

## STUDY ON ELECTROLYTIC REDUCTION WITH CONTROLLED OXYGEN FLOW FOR IRON FROM MOLTEN OXIDE SLAG CONTAINING FeO

Y.M. Gao<sup>a,\*</sup>, B. Wang<sup>a</sup>, S.B. Wang<sup>a</sup>, S. Peng<sup>a</sup>

<sup>a</sup> Key Laboratory for Ferrous Metallurgy and Resources Utilization of Ministry of Education, Wuhan University of Science and Technology, Wuhan, China

(Received 12 January 2012; accepted 25 June 2012)

### Abstract

A ZrO<sub>2</sub>-based solid membrane electrolytic cell with controlled oxygen flow was constructed: graphite rod / [O]<sub>Fe+C saturated</sub> / ZrO<sub>2</sub>(MgO)/(FeO)<sub>slag</sub> / iron crucible. The feasibility of extraction of iron from molten oxide slag containing FeO at an applied voltage was investigated by means of the electrolytic cell. The effects of some important process factors on the FeO electrolytic reduction with the controlled oxygen flow were discussed. The results show that: solid iron can be extracted from molten oxide slag containing FeO at 1450 °C and an applied potential of 4V. These factors, such as precipitation and growth of solid iron dendrites, change of the cathode active area on the inner wall of the iron crucible and ion diffusion flux in the molten slag may affect the electrochemical reaction rate. The reduction for Fe<sup>2+</sup> ions mainly appears on new iron dendrites of the iron crucible cathode, and a very small amount of iron are also formed on the MSZ (2.18% MgO partially stabilized zirconia) tube/slag interface due to electronic conductance of MSZ tube. Internal electronic current through MSZ tube may change direction at earlier and later electrolytic reduction stage. It has a role of promoting electrolytic reduction for FeO in the molten slag at the earlier stage, but will lower the current efficiency at the later stage. The final reduction ratio of FeO in the molten slag can achieve 99%. A novel electrolytic method with controlled oxygen flow for iron from the molten oxide slag containing FeO was proposed. The theory of electrolytic reduction with the controlled oxygen flow was developed.

**Keywords:** Oxygen-ion membrane; Electrolytic reduction; Controlled oxygen flow; Molten oxide slag; Iron

### 1. Introduction

Currently, the most important way to ironmaking and steelmaking is still that hot metal is obtained by carbon-based reduction of iron ore in the blast furnace, and then refined into steel by oxidation in the converter. This process would inevitably emit large quantities of CO<sub>2</sub> greenhouse gas. It is well known that high-temperature direct electrolysis is a basic method to produce some metals and alloys [1-5]. To solve thoroughly the problem of CO<sub>2</sub> emissions in ironmaking process, several researchers have explored direct electrolysis to prepare iron in recent years, such as the molten salt electrolysis method of G. Haarberg [6] and G.M. Li [7], and the molten oxide electrolysis method of D.R. Sadoway [8-10], et al. However, these electrolytic methods could cause some problems such as low current efficiency, more side effects, difficult to control the applied voltage, and even molten salt (slag) medium itself electrolyzed [7], etc.

In order to overcome these shortcomings of the

conventional electrolysis, a ZrO<sub>2</sub>-based solid membrane with strong selective permeability for the oxygen ions was employed to constitute the electrolytic cell and isolate the cathode and the anode during electrolysis. Oxygen ions from the molten salt (slag) could be transferred through the ZrO<sub>2</sub>-based oxygen-ion membrane by varying the chemical potential difference and applying an external voltage between the electrodes. Thus, an electrolytic method with controlled oxygen flow [11] was built up. As a novel emerging green metallurgical technique, the electrolysis with controlled oxygen flow has many advantages such as short process, high electrolytic efficiency, with emission of O<sub>2</sub> and so on. U.B. Pal and his co-workers have extracted some metals such as Mg [12], Ta [13] and Ti [14] from molten salt medium by utilizing this principle. Y. M. Gao [15,16] has obtained Fe from SiO<sub>2</sub>-CaO-Al<sub>2</sub>O<sub>3</sub>-FeO slag by external short-circuit galvanic cell. In this work, an external voltage was attempted to apply on the electrolytic cell with controlled oxygen flow to extract iron from SiO<sub>2</sub>-CaO- Al<sub>2</sub>O<sub>3</sub>-MgO-FeO slag.

\* Corresponding author: gym\_1@sina.com

## 2. Experimental principle

Molten oxide slag can be regarded as an ionic melt including oxygen ions and metal ions. The schematic diagram for electrolytic reduction with controlled oxygen flow is shown in Fig. 1. When the applied voltage between the electrodes exceeds the dissociation potential of the electro-active oxide in the molten slag, oxygen ions are pumped out of the slag through the oxygen-ion membrane and are oxidized at the membrane/anode interface, metal ions are reduced at the cathode. In order to investigate the feasibility of extraction of iron from the molten oxide slag containing FeO at the applied voltage, a carbon-saturated molten iron contained inside the MSZ tube instead of an inert anode is used as a consumable carbon anode in this study, the electrolytic cell system is constructed as follows: graphite rod | [O]Fe+C<sub>sat</sub> | ZrO<sub>2</sub>(MgO) | (FeO)<sub>slag</sub> | iron crucible. CO gas bubbles are evolved at the anode and pure iron is obtained at the cathode.

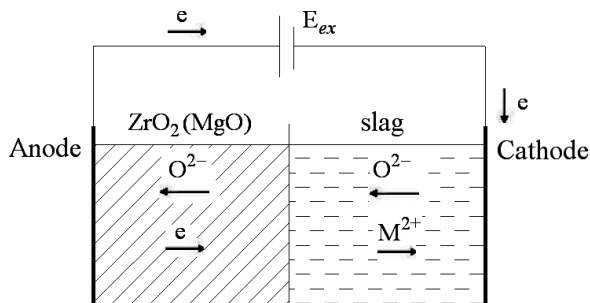


**Figure 1.** Schematic for electrolytic reduction with controlled oxygen flow  
Anode reaction:  $[C] + O^{2-} = CO + 2e$   
Cathode reaction:  $M^{2+} + 2e = M$

## 3 Experimental

### 3.1 Slag preparation

The composition of the master slag selected was 58%SiO<sub>2</sub>-25%CaO-10%Al<sub>2</sub>O<sub>3</sub>-7%MgO (mass fraction), and the corresponding position point A in the phase diagram [17] was shown in Fig. 2. The slag at A position, which was with low melting point of 1226°C (estimated by the FactSage thermodynamic software [18]) and low erosion against MSZ tube [19], helped to improve electrolytic reduction. The master slags were prepared from analytical reagent SiO<sub>2</sub>, CaO, Al<sub>2</sub>O<sub>3</sub>, and MgO powders mixed at components proportions. The FeO was prepared by heating FeC<sub>2</sub>O<sub>4</sub>·2H<sub>2</sub>O under high purely Ar (99.999%) and examined by X-ray Diffraction (XRD). In experiment 1, the slag was prepared by mixing the FeO into the master slag with the mass

ratio of FeO to master slag equal to 20:80. Experiment 2 was the blank test without FeO.

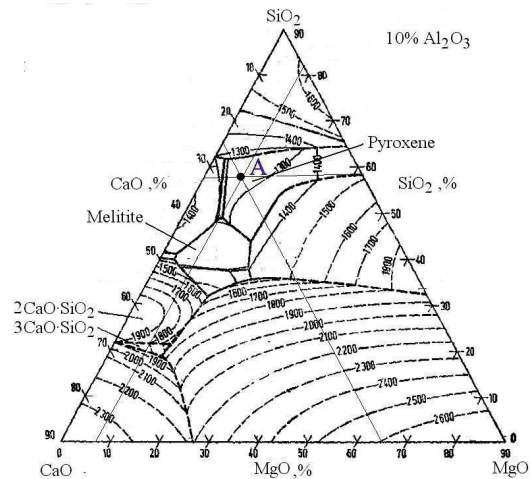


**Figure 2.** Phase diagram of CaO-MgO-SiO<sub>2</sub> containing Al<sub>2</sub>O<sub>3</sub> 10% (mass fraction)

### 3.2 Experimental process

The experiment was performed in two steps: first premelting slag material, and then the electrolysis experiment.

The slag with the mass of 18.00 g was put into a pure iron crucible (high 50mm, depth 45mm, inside diameter 20mm, outer diameter 30mm). A corundum crucible containing the pure iron crucible was placed within corundum furnace tube of a MoSi<sub>2</sub> resistance furnace. A 300 mL/min flow of purified Ar gas (by passing through thin copper wires and magnesium chips at 580°C) was introduced from the bottom of furnace tube. A graphite sleeve was surrounded in the upper of corundum furnace tube. The Ar gas and the graphite sleeve were used to prevent oxidation of both the slag and the iron crucible. A Pt-6%Rh/Pt-30%Rh thermocouple (type B) was employed to determine the experimental temperature. After the furnace was heated to 1400 °C, the slag sample was allowed to melt for 60 min. Then the iron crucible was taken out, and rapidly quenched in water, and then dried pre-slag material to reserve.

The electrolysis experimental apparatus was schematically shown in Fig. 3. The furnace configurations for electrolysis experiment were basically the same as that for the above slag premelting operation. In addition, a one-end-closed MSZ tube (inside diameter 7mm, outside diameter 10mm, length 78mm) was served as oxygen-ion membrane to separate the anode (Fe-C<sub>sat</sub> melt side) and the cathode (the molten oxide slag side) at high temperature. Fe-C<sub>sat</sub> melt was prepared by mixing about 4.5g iron powders and 0.5g graphite powders

inside the MSZ tube. A thin graphite rod with diameter 4mm and length 100mm was in contact with Fe-C<sub>sat</sub> melt during electrolysis. The thin graphite rod, together with the thick graphite rod with diameter 7mm and length 500mm that connecting with a molybdenum wire (diameter 1mm) was served as an anode lead. The pure iron crucible which contained the pre-made slag was directly used as the cathode. A pure iron rod with a corundum protection tube was linked to the iron crucible as a cathode lead. The upper alumina lid of the pure iron crucible was perforated in the middle position, so that the MSZ tube could drill through to fasten in the center of the pure iron crucible. For the convenience of operation, the MSZ tube was extended with a long corundum tube (inside diameter 11mm, length 800mm) by high temperature cement.

The molybdenum wire and the pure iron rod were respectively connected with CHI1140A electrochemical analyzer controlled by a computer program, the applied voltage for experiment was set to 4V, the interval and sensitivity scale of the acquisition data was set to 1s and 0.2 A/V, respectively. The filter was chosen with automatic setting. After the furnace was heated at a rate of 5°C/min to 1450°C, the slag sample was allowed to melt for 30 min. Switched on CHI1140A, the thin graphite rod lead of the anode was inserted into the Fe-C<sub>sat</sub> melt, and a half cell was made up. Then the half cell was immersed in the molten slag, the electrolytic cell was made up. Here the bottom of the MSZ tube should not touch the bottom of the pure iron crucible. The curve of the external current to the time was recorded in-situ by the CHI1140A electrochemical measurement system. The experiment was completed when the external current reached to a residual value with little variation. Experiment 2 was the blank with no FeO slag, the experiment process was the same as that of the experiment 1. After the experiment, the samples were observed with Nova 400 Nano SEM

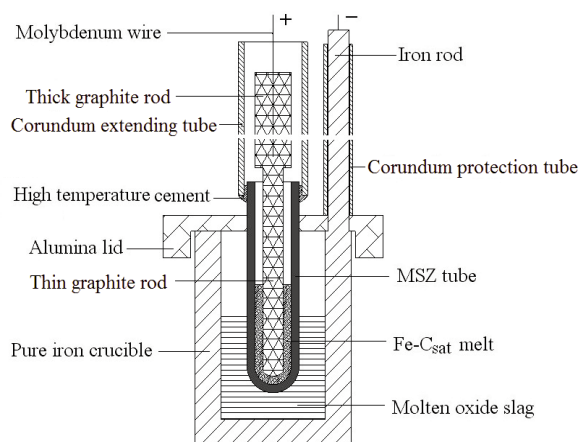


Figure 3. The electrolysis experiment device diagram

(Scanning Electron Microscopy) and EDS (Energy Disperse Spectroscopy) analysis.

### 3.3 Calculation for the FeO reduction ratio

Assuming that FeO in the molten slag is the only electro-active oxide, according to the Faraday's law, the reduction ratio of FeO in the molten slag at different times can be calculated with the following formula (1):

$$R = 100 \times \frac{M_{\text{FeO}} \int_0^t I_{\text{ion}} dt}{nmw_{\text{FeO}}F} \quad (1)$$

Where  $n$  the number of electrons taking part in the electrode reactions,  $n=2$  in the present case;  $F$  the Faraday constant,  $F=96500$  C/mol;  $I_{\text{ion}}$ -the reduction oxygen ionic current in the ionic membrane, A;  $t$  the reduction time, s;  $m$  the slag mass,  $m=18.00$ g;  $w_{\text{FeO}}$  the initial mass fraction of FeO in the molten slag,  $w_{\text{FeO}}=20\%$ ;  $M_{\text{FeO}}$  the molecular mass of FeO,  $M_{\text{FeO}}=72$  g/mol;  $R$  the reduction ratio of FeO in the molten slag, %.

## 4. Results and discussion

### 4.1 Analysis of the SEM images

The microstructures of the residual specimens were observed with a SEM after the experiment (Fig. 4). The SEM image of a slag/iron crucible interface is shown in Fig. 4(a). A lot of dendrites represented pure iron (confirmed by the EDS analysis) are full of inner slag adjacent to the iron crucible cathode. Solid Fe dendrites exist mainly around on the inner wall of the iron crucible cathode and there are no Fe dendrites in the middle region of slag away from the iron crucible wall. Under an applied voltage, oxygen ions in the molten slag migrated through the MSZ tube to the iron-carbon melt anode and were oxidized, CO gas bubbles were evolved and electrons were released. Fe<sup>2+</sup> ions migrated to the iron crucible wall cathode, then obtained electrons to precipitate solid Fe dendrites on the iron crucible wall, the new solid dendrites might become automatically new cathode locations; more Fe<sup>2+</sup> ions would continue to get electrons at the new locations to form more new solid Fe dendrites. On the one hand, Fe<sup>2+</sup> ions in the molten slag migrated and enriched to the cathode region; on the other hand, there were no iron precipitation in the middle slag region due to no enough electrons or Fe<sup>2+</sup> ions. Based on the iron crucible wall, solid Fe dendrites continuously grew and extended into the molten slag, interconnected and converged to groups until Fe<sup>2+</sup> ions were completely reduced.

The SEM image of the MSZ tube/slag interface is shown in Fig. 4(b). Some small iron beads are found near the MSZ tube/slag interface, the same phenomenon was also observed in the short-circuit

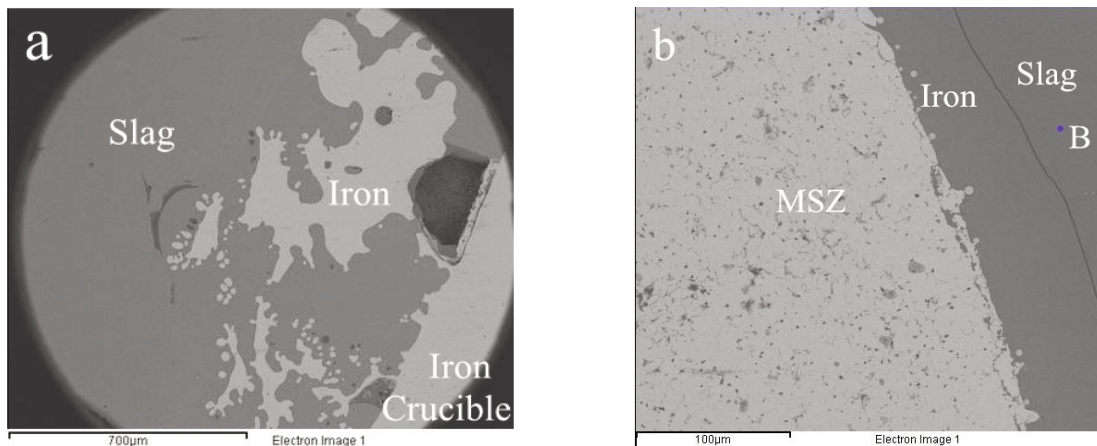


**Figure 4.** The SEM images of the residual specimens: (a). SEM image of slag/iron crucible interface, (b). SEM image of MSZ tube/slag interface

reduction [16, 20, 21]. This is because the MSZ tube is the oxygen-ion conductor with a certain electronic conductivity in nature. Not all electrons generated in the iron-carbon melt side reached the crucible cathode through the external circuit, but a small amount of electrons directly passed through the MSZ membrane to the MSZ tube/slag interface, the adjacent  $\text{Fe}^{2+}$  ions at the interface could gain these electrons and were reduced to iron beads.

Two transport paths of the electrons generated in the iron-carbon melt side could be concluded that: (1) The electrons transported from the anode to the cathode through the external circuit, a large number of Fe dendrites were formed around the iron crucible wall; (2) A small part of the electrons directly passed to the MSZ tube/slag interface through the MSZ membrane, and some little Fe beads were formed around the interface, but Fe bead amount was limited by the number of adjacent  $\text{Fe}^{2+}$  ions in the molten slag.

#### 4.2 Analysis of the curve of external current to time

The curves of the external current to time of experiment 1 and experiment 2 are shown in Fig. 5, respectively. The curve 1 of experiment 1 with the slag containing 20% FeO can be divided into three stages. At stage 1, the current gradually increases about 1.5 hours before reaching the peak. At the beginning of the reaction, the active cathode area of smooth iron crucible wall for  $\text{Fe}^{2+}$  ions electrochemical reduction was actually small, less  $\text{Fe}^{2+}$  ions were directly reduced on the iron crucible wall and less Fe dendrites were formed, that was why electrochemical reaction was slow and the external current was small at the initial stage. The distribution of  $\text{Fe}^{2+}$  ions around the prominent places of the Fe dendrites could be regarded as the nearly spherical, the growth rate for the spherical parts of the dendrite

was much faster than that for other positions (such as the iron crucible wall). Magnitude of curvature radius of dendrite tips was generally much smaller than the average diffusion layer thickness, so the diffusion flux at the tip position was much greater than that at other positions with the approximate plane, and this was in favor of larger current density and dendrites forming [22]. It can also be seen from Fig. 4(a), the quantity of Fe dendrites precipitated directly on the iron crucible wall is small, but that on the new Fe dendrites is very large. This indicates Fe precipitating on the new Fe dendrites is easier than on the iron crucible wall. Once Fe dendrites were precipitated on the iron crucible wall, there would be more Fe precipitation on the Fe dendrites, so the growth rate of Fe dendrites could be sped up, while the active cathode area were increased significantly. Therefore, the electrochemical reduction could be accelerated and the external current be increased till the maximum current value. A similar phenomenon had also been observed during electrolysis [23]. At stage 2, the current gradually decreases from the peak. With the reduction of FeO in the molten slag, the active cathode area had been great as it was already due to precipitation of Fe dendrites at stage 1, but now with the decrease of the FeO concentration in the molten slag, the FeO activity [18] and the slag conductivity [24] decreased. Simultaneously the slag viscosity increased [17], the ion diffusion flux decreased, thus the oxygen-ion current decreased, and the external current decreased. At stage 3, after the first two stages of electrochemical reduction, the FeO concentration in the molten slag was quite low, the current reached to a residual value with little variation, which indicated that the reduction reaction was close to complete at this stage.

The curve 2 mainly reflects the background current caused by some effects such as the reduction of impurities in the molten slag, "leakage" current [12] which directly passes from the cathode to the

anode through the slag and the MSZ tube, and the resistance furnace electromagnetic fields, etc.

Also can be seen in Fig. 5, the residual current of the experiment 1 is larger about 0.1A than the blank experiment 2. It may be due to a change of the conduction mechanism nature of MSZ tube. During electrolysis the current could cause an increase of the electronic conductivity of the MSZ tube [14] in experiment 1 with FeO in the slag. Since there was no FeO in the slag in experiment 2, a very small current passed through the MSZ tube, the conductivity of the MSZ tube should have little change before and after experiment. Therefore, the changes of the MSZ tube conductivity were different in the two experiments. Here the conventional blank test (experiment 2) is not suitable for determining the current efficiency as a reference standard.

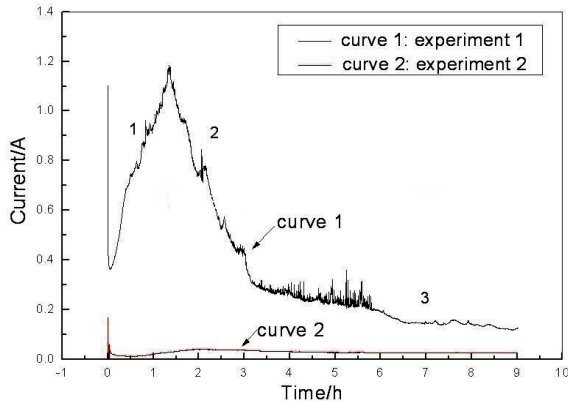


Figure 5. Curves of external current to time at applied potential of 4V

### 4.3 Equivalent circuit analysis

The reduction rate of FeO in the molten slag is closely related to the oxygen-ion current which passes through the oxygen-ion membrane, the equivalent circuit of the solid electrolyte was often used to analyze conduction mechanism by several researchers. According to the literature [12], the equivalent circuit for the present experimental can be shown in Fig. 6. The characteristics of slag electrochemical reduction process and the current expressions can be analyzed.

Fig. 4(b) shows that there are some iron beads reduced from the slag around the MSZ tube/slag interface, thus it can be concluded some electrons generated in the carbon saturated iron melt side directly passed through the MSZ tube into the slag in the initial period of the reaction. The direction of the above electron current is opposite with the shown in the Fig. 6, and apparently the current relationship is:

$$I_{ion} = I_{ex} + I_e \quad (2)$$

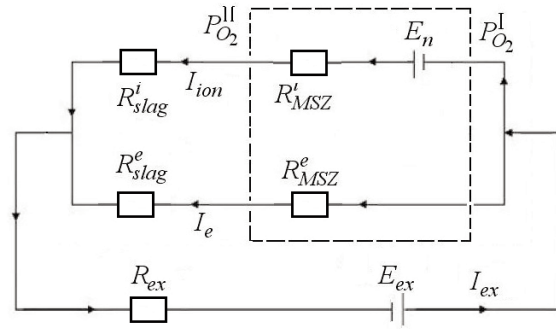


Figure 6. Equivalent circuit of electrolytic reduction with controlled oxygen flow

$E_n, E_{ex}$  -the Nernst potential and applied voltage, respectively;  $R_{MSZ}^i, R_{slag}^i$  -the oxygen ionic resistance in the ionic membrane and the ionic resistance in the molten slag, respectively;  $R_{MSZ}^e, R_{slag}^e$  -the electronic resistance in the ionic membrane and the slag, respectively;  $R_{ex}$  -the external circuit resistance;  $I_e$  -the electronic current in the ionic membrane;  $I_{ex}$  -the external circuit current;  $P_{O_2}^I$  -the oxygen partial pressure in the carbon saturated iron melt;  $P_{O_2}^{II}$  -the oxygen partial pressure in the molten slag.

Here the electronic current  $I_e$  can promote the FeO reduction. However, under an applied voltage, the  $Fe^{2+}$  ions would move to the cathode side, the electron flow, which directly passed through the MSZ tube into the molten slag, would be blocked by non-FeO slag with very small electronic conductivity after the  $Fe^{2+}$  ions near the MSZ tube/slag interface were depleted. With the FeO concentration decrease, slag conductivity decreased [24] and the electronic conductivity of MSZ tube also changed [14]. Under the applied electric field, there would be a part of electrons from the cathode through the slag into the MSZ tube directly to the anode (like “leakage” current [12]), which led to electronic current reverse as shown in Fig. 6, the current relationship is:

$$I_{ex} = I_{ion} + I_e \quad (3)$$

Here the electronic current  $I_e$  did not only play no reduction role, but decreased the efficiency of applied voltage. With the reduction of FeO, the oxygen-ion current  $I_{ion}$  in theory would gradually decrease to near 0. Finally, the external circuit current  $I_{ex}$  was equal to the electronic current  $I_e$ . They could be regarded as the residual current, which indicated the FeO reduction had been basically completed.

It can be figured from the above, the current efficiency would be improved only when the ionic conduction of the MSZ tube and the molten slag increased, the electronic conduction decreased, even blocked off.

#### 4.4 The FeO reduction ratio analysis

During the slag reduction process, the oxygen-ion current  $I_{\text{ion}}$  and the electronic current  $I_e$  could not be measured directly. In consideration of the  $I_e$  is generally small, and it is opposite direction in the earlier and the later stage of the electrolysis, one can adopte  $I_{\text{ion}}=I_{\text{ex}}$  to calculate  $I_{\text{ion}}$  when  $I_e$  is neglected. From the above analysis, the residual current should be deducted from  $I_{\text{ex}}$  when calculating the reduction ratio. One can obtain the curve of the FeO reduction ratio to time as shown in Fig. 7 in accordance with formula (1). Comparing with Fig. 5, the reduction ratio increased rapidly at the beginning stage; 3 hours later, the reduction ratio increased slowly, the final reduction ratio calculated is about 88.5%.

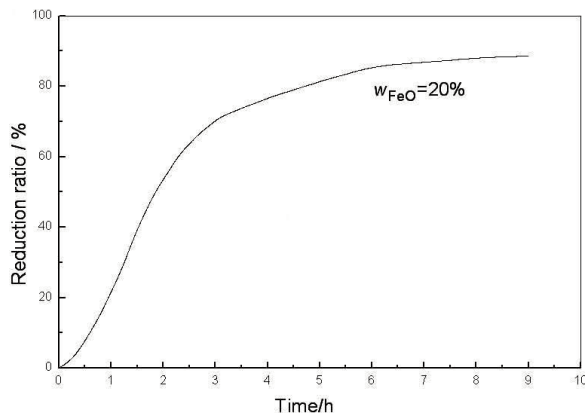


Figure 7. Curve of the FeO reduction ratio in the molten slag to time

The color of the residual slag was found to become very light after experiment 1. The EDS analysis results for point B in Fig. 4(b) are listed in Table 1, which indicates that very small amount of FeO in the slag were not reduced yet. The final average reduction ratio of FeO in the molten slag was estimated to be 99%. The final reduction ratio calculated by the formula (1) was lower than that by the EDS analysis, this was because the former ignored the reduction role by the internal electronic current which passed directly through the MSZ tube.

Table 1. The EDS analysis of point B location in Fig.4(b)

Elements	O	Mg	Al	Si	Ca	Fe	Totals
Mass%	43.34	1.69	5.28	33.62	14.83	1.24	100

#### 5. Conclusions

(1) Metal iron could be extracted from the molten oxide slag containing FeO by means of electrolysis with controlled oxygen flow at 1450°C and applied voltage of 4V. Solid iron mainly existed in the form of

iron dendrites which distributed around the inner wall of the iron crucible cathode, a small amount of iron beads distributed around the MSZ tube/slag interface, but there was no metal iron in the middle slag region.

(2) During electrolysis with controlled oxygen flow for iron, iron dendrites' precipitation and growth could lead to the cathode active area increasing significantly, promote the electrochemical reduction reaction. After the current reached to the extreme value, the rate of electrochemical reaction would decrease with a decrease of the ion diffusion flux in the molten slag.

(3) The electronic current through the MSZ tube played a different role at the early and the later period during the electrochemical reduction of FeO in the molten slag. The electronic conductivity of the oxygen-ion membrane could promote the reduction of FeO at the early period, but reduce the current efficiency at the later period. The key to improve the current efficiency is to increase the ionic conductivity of the slag and the oxygen-ion membrane, and decrease their electronic conductivity.

(4) The total reduction ratio of FeO in the molten slag included: reduction caused by external circuit current, as well as the reduction of the internal electronic current caused by the electronic conductivity of the oxygen-ion membrane. The final actual reduction ratio of FeO was about 99%.

#### Acknowledgement

The authors acknowledge the project funds provided by the National Natural Science Foundation of China (No.51174148).

#### References

- [1] G Z Chen, D J Fray, T W Farthing, Nature, 407(6802)(2000)361-364.
- [2] G. Kaptay, J. Min. Metall. Sect. B-Metall. 39 (1-2) B (2003) 1-2.
- [3] R. Shi, C. Bai, M. Hu, X. Liu and J. Du, J. Min. Metall. Sect. B-Metall. 47 (2) B (2011) 99-104.
- [4] T. P. Jose, L. Sundar, L. J. Berchmans, A. Visuvasam and S. Angappan, J. Min. Metall. Sect. B-Metall. 45 (1) B (2009) 101-109.
- [5] W Xiao, H Zhu, H Y Yin, D H Wang. Journal of Electrochemistry, 18(3) (2012)193-200 (in Chinese).
- [6] G. Haarberg, O. Burheim, D. Fray, S. Male, VIII International Conference on Molten Slags, Fluxes & Salts, January 18-21, Santlago, Chile, 2009, p.1425-1433.
- [7] G.M. Li, D.H. Wang, Zhen Chen, J. Mater. Sci. Technol, 6(25) (2009) 767-771.
- [8] A.H.C. Sirk, D.R. Sadoway, L. Sibille, ECS Transactions, 28 (6) (2010)367-373.
- [9] D.H. Wang, A.J. Gmitter, D.R. Sadoway, Journal of the Electrochemical Society, 158 (6) (2011) E51-E54.
- [10] H.J. Kim, J. Paramore, A. Allanore, D.R. Sadoway,

- Journal of the Electrochemical Society, 158 (6) (2011) E101-E105.
- [11] Y.M. Gao, Y. Jiang, H. Zhang, X.M. Guo and K.C. Chou, *Journal of Wuhan University of Science and Technology*, 30(5) (2007) 449-453(in Chinese).
- [12] A.Krishnan, X.G. LU, U.B. Pal, *Metallurgical and Materials Transactions*, 8(36) B (2005) 463-473.
- [13] A. Krishnan, X.G. LU, U.B. Pal, *Scandinavian Journal of Metallurgy*, 34(2005) 293-301.
- [14] M. Suput, R.D. Lucas, S. Pati, G. Ye and U. Pal, A.C. Power, *Mineral Processing and Extractive Metallurgy*, 117(2) (2008) 118-122.
- [15] Y.M. Gao, X.M. Guo, K.C. Chou, *Acta Metallurgica Sinica*, 42(1) (2006) 87-92 (in Chinese).
- [16] Y.M. Gao, X.M. Guo, K.C. Chou, *Journal of University of Science and Technology Beijing*, 11 (4) (2004) 306-309.
- [17] Association of Germany Iron and Steel Engineer, translated by J. Wang, Y.Q. Peng, Y.W. Mao, *Schlackenatlas Slag Atlas*, Metallurgical Industry Press, Beijing, China, 1989, p.103 and 282 (in Chinese).
- [18] C.W. Bale, E. Belisle, P. Chartrand, S.A. Decterov and G. Eriksson, *Computer Coupling of Phase Diagrams and Thermochemistry*, 33 (2009) 295-311.
- [19] Yau-Don Chung, Mark E. Schlesinger, *Journal of the American Ceramic Society*, 77(3) (1994) 611-616.
- [20] Y.M. Gao, X.M. Guo, S. Gan, K.C. Chou, *Journal of Iron and Steel Research*, 17(2) (2005) 19-23 (in Chinese).
- [21] Y.M. Gao, X.M. Guo, K.C. Chou, *The Chinese Journal of Nonferrous Metals*, 16(3) (2006) 530-535 (in Chinese).
- [22] H.T. Guo, S.W. Yao, *The Electrochemical and Measurement Basis*, Chemical Industry Press, Beijing, China, 2009, p.186 (in Chinese).
- [23] Y.C. Chen, X.G. Lu, Q. Li, H.W. Cheng, *Rare Metal Materials and Engineering*, 36(11) (2007) 1991-1995 (in Chinese).
- [24] C.Y. Sun, X.M. Guo. *Trans. Nonferrous Met. Soc. China*, 21 (2011) 1648-1654.